



A Deep Two-Stage Scheme for Polycrystalline Micro-Crack Detection

Sirui Chen[†]

Key Laboratory of Measurement
and Control of CSE, Ministry of
Education, School of Automation
Southeast University
Nanjing, China
inchensirui@126.com

Shuo Shan

Key Laboratory of Measurement
and Control of CSE, Ministry of
Education, School of Automation
Southeast University
Nanjing, China
seu_shuoshan@outlook.com

Liping Xie

Key Laboratory of Measurement
and Control of CSE, Ministry of
Education, School of Automation
Southeast University
Nanjing, China
lpxie@seu.edu.cn

Haikun Wei

Key Laboratory of Measurement and
Control of CSE, Ministry of
Education, School of Automation
Southeast University
Nanjing, China
hkwei@seu.edu.cn

Jinxia Zhang

Key Laboratory of Measurement and
Control of CSE, Ministry of
Education, School of Automation
Southeast University
Nanjing, China
Industrial Robot Application of
Fujian University Engineering
Research Center
Minjiang University
Fuzhou, China
jinxiazhang@seu.edu.cn

ABSTRACT

Solar cell efficiency is one of the most concerned issues during the photovoltaic power generation. The existed micro-crack detection approaches mainly rely on manual work with the detection efficiency is low. Besides, there lacks exploration in algorithms for separating the region of damage without much workforce. In this paper, we propose a two-stage deep scheme, especially for the polycrystalline micro-crack detection method. A region of interest (ROI) proposal method based on the canny feature and the wavelet feature for micro-crack is raised. The computational efficiency and detection accuracy are greatly improved. Firstly, we split the original electroluminescent image (EL image) by its grid line and cut them into fixed-size squares. Then the ROI proposal method is applied to extract candidate boxes as the inputs of the second stage. At the second stage, a modified convolution neural network based on the candidate boxes is supervised by binary labels. Our experimental results demonstrate that our polycrystalline micro-crack detection scheme outperforms other traditional frameworks.

Permission to make digital or hard copies of all or part of this work for personal or classroom use is granted without fee provided that copies are not made or distributed for profit or commercial advantage and that copies bear this notice and the full citation on the first page. Copyrights for components of this work owned by others than ACM must be honored. Abstracting with credit is permitted. To copy otherwise, or republish, to post on servers or to redistribute to lists, requires prior specific permission and/or a fee. Request permissions from Permissions@acm.org.

PRIS 2020, July 30-August 2, 2020, Athens, Greece
© 2020 Association for Computing Machinery.
ACM ISBN 978-1-4503-8769-9/20/07...\$15.00
<https://doi.org/10.1145/3415048.3416119>

This work is the first attempt to solve engineering problems about micro-crack by deep learning techniques in photovoltaic systems, without many high-quality labels and computing power.

CCS CONCEPTS

•Software and its engineering •Applied computing~Operations research~Computer-aided manufacturing

KEYWORDS

Poly-crystalline photovoltaic panel, Micro-crack, ROI, CNN

1 Introduction

In recent years, energy and environmental issues highlight the importance of photovoltaic power generation [1]. Meanwhile, the solar cell is the core component of photovoltaic power generation technology. Solar panels can be divided into monocrystalline and polycrystalline panels. Micro-crack and broke gate [2] are the two typical damage and we mainly focus on the micro-crack. Apparently, damages will directly reduce the power efficiency, reliability, and even the stability of photovoltaic power generation. Usually, in industrial sites, damage detection is also used as an essential evaluation basis for photovoltaic power generation efficiency [3]. However, manual identification is mostly adopted in actual production.

Micro-crack on photovoltaic panels is invisible without EL images. There are several difficulties in the detection of micro-crack. Firstly, crack is difficult and time-consuming to be distinguished due to the floccule. Secondly, the grid line on the panels is probably to result in ambiguity to micro-crack in detection. Thirdly, due to not only the imbalance between positive and negative examples but also the requirements of positioning accuracy, the direct detection of the whole EL image is inefficient and cannot satisfy the demand.

Owing to the above problems, we propose a deep two-stage scheme for polycrystalline micro-crack detection. At the first stage, we have an improved screening strategy to extract five ROI on each piece. At the second stage, a modified convolution neural network based on the both ROI and original image features is supervised by binary labels [4, 5]. After the comparison experiments, we conclude that the proposed deep two-stage scheme for polycrystalline micro-crack detection has achieved better results. The critical contributions of our work are as follows:

- Compared with Fast R-CNN, a more effective ROI extraction method is designed for the micro-crack detection.
- Our approach outperforms than traditional machine learning methods. The reason is that it focuses ROI on the object as much as possible and excludes other irrelevant information.
- This work is the first attempt to solve engineering problems about micro-crack by deep learning techniques in photovoltaic systems, without many high-quality labels and computing power.

2 Related Work

2.1 Object detection

Object detection dates back for a long time and springs up an abundance of approaches [6, 7]. Classical work [8, 9, 10] usually formulated object detection as a sliding window classification problem. Usually, the algorithm has been SVM or RF [11]. However, these methods were challenging to extract deep semantic information of some images, and the time complexity was high. Deep learning methods based on ROI are an essential branch in object detection [12]. Region-based CNNs (R-CNN) extracted ROI by selective search, and a detection network was trained to classify each ROI independently [13]. The drawback lied in that time cost of the ROI generation algorithm was high. It was extended by Fast R-CNN [14]. The methods mentioned above are mainly designed for the salient object while the micro-crack tends to be confused with the polycrystalline materials. As a result, there remain problems of not combining the feature of specific objects when detected by the methods mentioned before.

2.2 Industrial background of micro-crack detection

Resonance ultrasonic vibrations (RUV) method for crack detection in Photovoltaic (PV) silicon wafers has been firstly proposed by [15]. The photoluminescence (PL) detection method was first developed to enhance the detection of solar cell micro-cracks.

Another predominantly used method of micro-cracks detection is Electroluminescence (EL) [16]. The mainstream detection of micro-crack in solar panels is based on the acquisition of EL images. However, the detection work of polycrystalline micro-crack still relies on manual discrimination due to the polycrystalline materials.

3 Methodology

In this chapter, we will introduce the whole process of the micro-crack detection method, which are pre-processing, region proposal and our micro-crack detection network [17].

3.1 Pre-processing

There are 42 images in total. First, the distortion of the EL image is corrected. We cut the image of the cells according to the boundary and obtain a total of 42*72 pieces of images with size 40*240. Finally, 19298 images of size 40*40 are made. The number of cracks and non-crack images is about 10:1. The usual approaches of data augmentation are random crop, horizontal/vertical flip, shift and rotation or reflection [18]. After data augmentation, the ratio of positive to negative samples is about 1:1. The Haar wavelet is used to extract the low-frequency features of the original image, while the high-frequency image is discarded. Low-frequency wavelet image can effectively filter the high-frequency noise in the background and keep the micro-crack feature.

3.2 Region proposal

The expected ROI obtains local valid information, such as micro-crack and floccule. The purpose of ROI is to extract and fuse more local features, to facilitate subsequent convolutional neural network learning rules and improve the accuracy.

To begin with, we use the selective search to extract ROI and screened out some boxes according to the moderate size. For 40*40 images, if the contour is more massive than 140, the ROI should be abandoned because it almost contains global information. Similarly, if the outline is too small, it does not satisfy the requirement. Next, to make the areas contain more floccule or micro-crack features, we combine the edge information to conduct a secondary screening of ROI. The edge is obtained by the Canny algorithm, and 150 is chosen as the threshold after the experiment with different luminance. The effective information proportion E_{num}^k of the k ROI is larger than 25%:

$$E_{num}^k = \frac{N_{rec}^k}{N_{edge}} > 25\%, k = 1, 2, \dots, 5 \quad (1)$$

N_{rec}^k is the number of edge information of the k ROI. N_{edge} is the total number of edge information in each image. Or the effective size S_{num}^k of k ROI is bigger than 40%:

$$S_{num}^k = \frac{S_{rec}^k}{W_{rec}^k * H_{rec}^k} = \frac{N_{rec}^k}{W_{rec}^k * H_{rec}^k} > 40\% \quad (2)$$

W_{rec}^k and H_{rec}^k are the width and height of the k ROI. Edges are composed of pixels, so the number of edge pixels in an ROI equals the area. Only if the ROI satisfied (1) or (2), it can be kept. The ROI prioritization strategy follows in descending order:

- The area is greater than 40.
- When the mean pixel in the ROI is less than the mean pixel of the whole image, it is arranged in descending order of area and grayscale. If the area is the same, the ROI with more excellent gray value is preferred.
- The mean pixel of ROI is higher than the whole image.
- Experiments and analyses are conducted on several images to study the relationship between ROI number, area, medium gray of ROI and full image. Then an ROI priority strategy is developed. For images with more than 5 ROI, the top 5 ROI will be selected. While other situations, the ROI is added by the priority until 5 ROI is selected. The ROI is extracted by the following procedures in Table 1, and then they are sent into the micro-crack detection training network. Figure 1 shows the process of the whole region proposal.

Table 1. Experiment Procedures.

1. Cut images into small pieces (from 240×240 to 40×40).
 2. Enhance the negative data.
 3. Traverse each image:
 - Extract wavelet low-frequency image
 - Extract ROI by selective search on the **wavelet image**
- If the number of ROI > 5 :
Canny features and areas are prioritized for ROI.
Delete the tail of the queue until the queue length is 5.
- If the number of ROI < 5 :
Canny features and areas are prioritized for ROI.
Add the front of the queue until the queue length is 5.
- Obtain the top-left coordinates of the 5 ROI.

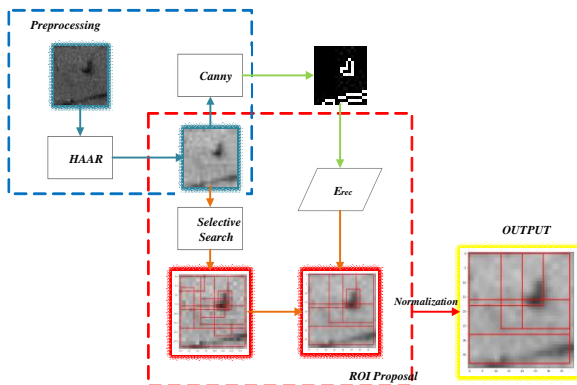


Figure 1: Region proposal.

3.3 Micro-crack detection network

The complete process is illustrated in Figure 2.

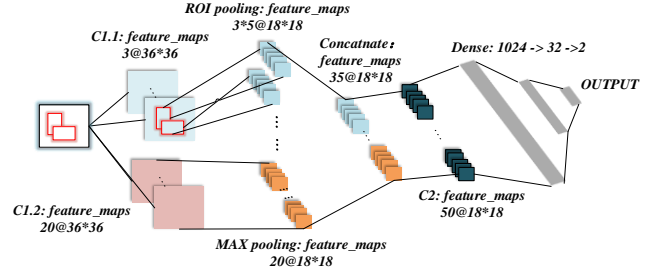


Figure 2: The Proposed Architecture.

After obtaining the ROI coordinates, we will not get the accuracy and the recall rate for each ROI. On the one hand, considering the small proportion of micro-crack in the whole figure, the accuracy rate of ROI will be biased. For example, in the negative sample, due to the small area of micro-crack, there is a certain probability that ROI is a positive sample. That is why the accuracy rate will be low, and the number of ROI is controlled. On the other hand, the ROI is only used as local features to integrate original image information in the binary network, which makes the system pay more attention to local information.

4 Experiment

In this part, the detection accuracy of our model and some common approaches will be demonstrated and compared. The detection result will be illustrated in the original image directly.

Different machine learning models were applied to compare the effects of our micro-crack detection scheme. We extracted four features of the image, which were hog feature, Fourier spectrum feature, LBP feature and Haar wavelet low-frequency feature [19]. The Multi-Layer Perception (MLP) and Support Vector Machine (SVM) were selected for comparison [20]. The input of MLP was the fusion of the LBP feature and Haar feature, the fusion of hog feature and Haar feature. While the input of SVM was the fusion of hog feature and Fourier feature, the fusion of hog feature and Haar feature.

The different features of each image were transposed after vertical splicing. The length of the feature was compressed from 80 to 30 utilizing principal component analysis (PCA). Then they were sent to the neural network for training. The experiment shows that more than 99% of information can be fully characterized after compression, which means the compression is feasible.

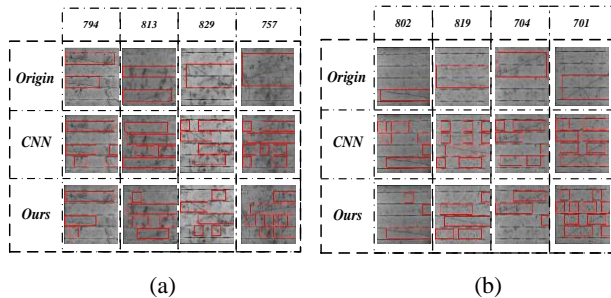
CNN was also chosen for the experiment, and we used two layers of convolution, one layer of pooling and two layers of full connection. The size of the convolution kernel template was 5. The reason for reducing the pooling layer is that the pooling will reduce the gradient information when the amount of computation is small [21].

Table 2: Accuracy in Different Models

Number	Structure	Accuracy	TP	TN
1	LBP+HAAR+SVM	51.5%	51.351%	51.656%
2	HOG+HAAR+SVM	52.98%	50.993%	54.967%
3	HOG+FOURIER+MLP	52.667%	46.667%	58.667%
5	HOG+HAAR+MLP	61.333%	55.998%	66.667%
6	CNN	83.05%	69.6%	96.5%
7	OURS	89.89%	89.5%	90.25%

After the comparison of Table 2, conclusions follow. TP means the proportion of positive samples that are classified rightly while TN represents the negative samples. The accuracy is the average of TP and TN. When it comes to 1 and 2, it can be found that since the hog feature integrates gradient information and pay more attention to the edge, so the TN in Model 1 is better than 2. Considering the uncertainty of no micro-crack information, which means the floccule, the effect of TP is not good. By comparing 3 and 4, the classification accuracy can be significantly raised in the wavelet low-frequency information, which makes us decide to seek ROI on the Haar image. The accuracy of MLP is much better than SVM. Therefore, the classical approach is infeasible in the scenario where the character is not apparent.

We also compared the classical CNN with the depth model adopting the improved ROI screening. It can be seen that the accuracy rate of micro-crack detection is up to 96%, which refers to the micro-crack images. However, the price of non-crack image detection is relatively low, which is only 69%. This is not an ideal result. Although the classifier can tell us whether the plate has micro-cracks, there is a great disturbance to the location of the target. In our proposed algorithm, even though the accuracy of negative samples is reduced by 5%, the recognition rate of the positive sample is necessarily increased, which means the overall efficiency is much higher.

**Figure 3: Detection Results of CNN and Our Model (a): more floccule (b): less floccule**

As shown in Figure 3, the parts identified as micro-cracks are marked with red boxes on each image to realize positioning. We selected two representative panels, (a) for the panel with more floccule, and (b) for the picture with cleaner background, to observe the effect of the algorithm for these two graphs.

Table 3: Mistaken detection results.

Index of Images	Origin Cracked Size	CNN		Our Model	
		S_p	S_n	S_p	S_n
794	25%	25%	11.11%	25%	2.78%
813	31.94%	31.94%	25%	25%	13.89%
829	30.56%	20.83%	23.61%	20.83%	9.72%
757	50%	38.89%	6.94%	29.17%	9.72%
802	15.28%	13.89%	18.06%	13.89%	2.78%
819	33.33%	22.22%	18.06%	23.61%	15.28%
704	30.56%	20.83%	13.89%	20.83%	2.78%
701	30.56%	26.39%	27.78%	20.83%	18.06%

The origin cracked size is the ratio of origin defect size to the image's full size. S_p is the ratio of detected micro-crack size S_{crack} to the full size S_{full} . S_n is the ratio of the mistakenly detected micro-crack size S_w to the full size S_{full} .

$$S_p = \frac{S_{crack}}{S_{full}} \quad (3)$$

$$S_n = \frac{S_w}{S_{full}} \quad (4)$$

These two methods can cover the crack area. However, as shown in **Table 3**, the false detection area of CNN is larger than that of our model, such as Image 794, Image 802 and Image 704. Therefore, both algorithms need to be improved.

5 Discussion

In this work, we propose a deep two-stage scheme for polycrystalline micro-crack detection based on ROI. The accuracy of crack detection can reach 89.89%. In practical engineering applications, the false detection rate is as important as the correct rate. Because the crack area is relatively small, less false detection rate is more important, so our algorithm is effective. Compared with other methods, it can locate the crack location better and reduce the area of false detection.

ACKNOWLEDGMENTS

This work was supported in part by the National Key Research and Development Program of China under Grant 2018YFB1500800, in part by the National Natural Science Foundation of China under Grant 61802059 and Grant 61773118 and Grant 61703100, in part by the Natural Science Foundation of Jiangsu under Grant BK20180365 and Grant BK20170692, in part by the Zhishan Young Scholar Program of Southeast University and the

Fundamental Research Funds for the Central Universities under Grant 2242020R40119, in part by the Fundamental Research Funds for the Central Universities and Industrial Robot Application of Fujian University Engineering Research Center, Minjiang University.

REFERENCES

- [1] S Eftekharijrad and G T Heydt and V Vittal July 2015 Optimal Generation Dispatch With High Penetration of Photovoltaic Generation *IEEE Transactions on Sustainable Energy* 6 1013-1020
- [2] S Johnston et al Jan. 2014 Correlating Multicrystalline Silicon Defect Types Using Photoluminescence, Defect-band Emission, and Lock-in Thermography Imaging Techniques *IEEE Journal of Photovoltaics* 4 348-354
- [3] H D Tafti and A I Maswood and G Konstantinou and J Pou and F Blaabjerg May 2018 A General Constant Power Generation Algorithm for Photovoltaic Systems *IEEE Transactions on Power Electronics* 33 4088-4101
- [4] J Li and X Liang and S Shen and T Xu and J Feng and S. Yan April 2018 Scale-Aware Fast R-CNN for Pedestrian Detection *IEEE Transactions on Multimedia* 20 985-996
- [5] R Girshick 2015 Fast R-CNN 2015 *IEEE International Conference on Computer Vision (ICCV)* 1440-1448
- [6] Q Hu and S Paisitkriangkrai and C Shen and A van den Hengel and F Porikli April 2016 Fast Detection of Multiple Objects in Traffic Scenes With a Common Detection Framework *IEEE Transactions on Intelligent Transportation Systems* 17 1002-1014
- [7] Liping Xie, Weili Guo, Haikun Wei, Yuanyan Tang, Dacheng Tao, Efficient Unsupervised Dimension Reduction for Streaming Multi-view Data, *IEEE Transactions on Cybernetics*
- [8] N Dalal and B Triggs 2005 Histograms of oriented gradients for human detection 2005 *IEEE Computer Society Conference on Computer Vision and Pattern Recognition (CVPR'05)* 1 886-893
- [9] P F Felzenszwalb and R B Girshick and D McAllester and D Ramanan September 2010 Object Detection with Discriminatively Trained Part-Based Models *IEEE Transactions on Pattern Analysis and Machine Intelligence* 32 1627-1645
- [10] P Viola and M Jones 2001 Rapid object detection using a boosted cascade of simple features *Proceedings of the 2001 IEEE Computer Society Conference on Computer Vision and Pattern Recognition I-I*
- [11] X Wu and W Zuo and L Lin and W Jia and D Zhang November 2018 F-SVM: Combination of Feature Transformation and SVM Learning via Convex Relaxation *IEEE Transactions on Neural Networks and Learning Systems* 29 5185-5199
- [12] Liping Xie and Dacheng Tao and Haikun Wei 2019 Early Expression Detection via Online Multi-instance Learning with Nonlinear Extension *IEEE Transactions on Neural Networks and Learning Systems (TNNLS)* 30 1486-1496
- [13] R Girshick and J Donahue and T Darrell and J Malik 2014 Rich feature hierarchies for accurate object detection and semantic segmentation *IEEE Computer Society Conference on Computer Vision and Pattern Recognition*
- [14] K He and X Zhang and S Ren and J Sun 2014 Spatial pyramid pooling in deep convolutional networks for visual recognition *European Conference on Computer Vision*
- [15] A Belyaev and O Polupan and W Dallas and S Ostapenko and D Hess and J Wohlgemuth February 2006 Crack detection and analyses using resonance ultrasonic vibration in full-size crystalline silicon wafers *Appl. Phys. Lett.* 88
- [16] M Köntges and M Siebert and D Hinken and U Eitner and K Bothe and T Potthof September 2009 Quantitative analysis of PV-modules by electroluminescence images for quality control *24th Eur. Photovoltaic Solar Energy Conf* 21-24
- [17] Chi Zhang, Haikun Wei, Liping Xie, Kanjian Zhang, Direct interval forecasting of wind speed using radial basis function neural networks in a multi-objective optimization framework, *Neurocomputing*, 2016, 205:53-63.
- [18] A Fawzi and H Samulowitz and D Turaga and P Frossard 2016 Adaptive data augmentation for image classification 2016 *IEEE International Conference on Image Processing* 3688-3692
- [19] Xin Wang September 2006 Moving window-based double haar wavelet transform for image processing *IEEE Transactions on Image Processing* 15 2771-2779
- [20] L. Xie, J. Zhao, H. Wei, K. Zhang and G. Pang, "Online Kernel-Based Structured Output SVM for Early Expression Detection," in *IEEE Signal Processing Letters*, vol. 26, no. 9, pp. 1305-1309, Sept. 2019.
- [21] C Lee and P Gallagher and Z Tu April 2018 Generalizing Pooling Functions in CNNs: Mixed, Gated, and Tree *IEEE Transactions on Pattern Analysis and Machine Intelligence* 40 863-875